Published in final edited form as:
*Cell Metab*. 2011 April 6; 13(4): 461–468. doi:10.1016/j.cmet.2011.03.004.

# PARP-1 inhibition increases mitochondrial metabolism through SIRT1 activation

**Péter Bai**[1,2], **Carles Canto**[3], **Hughes Oudart**[4], **Attila Brunyánszki**[2], **Yana Cen**[5], **Charles Thomas**[3], **Hiroyasu Yamamoto**[3], **Aline Huber**[1], **Borbála Kiss**[1], **Riekelt H. Houtkooper**[3], **Kristina Schoonjans**[3], **Valérie Schreiber**[1], **Anthony A. Sauve**[5], **Josiane Menissier-de Murcia**[1], and **Johan Auwerx**[3,*]

[1] IREBS, FRE3211-CNRS, Université de Strasbourg, ESBS, Illkirch, France [2] Department of Medical Chemistry, University of Debrecen, Debrecen, Hungary [3] Laboratory of Integrative and Systems Physiology, Ecole Polytechnique Fédérale de Lausanne, Switzerland [4] CEPE, CNRS UPR9010, Strasbourg, France [5] Department of Pharmacology, Weill Cornell Medical College, New York, NY, USA

## Summary

SIRT1 regulates energy homeostasis by controlling the acetylation status and activity of a number of enzymes and transcriptional regulators. The fact that $NAD^+$ levels control SIRT1 activity confers a hypothetical basis for the design of new strategies to activate SIRT1 by increasing $NAD^+$ availability. Here we show that the deletion of the poly(ADP-ribose) polymerase-1 (*PARP-1*) gene, encoding a major $NAD^+$-consuming enzyme, increases $NAD^+$ content and SIRT1 activity in brown adipose tissue and muscle. *PARP-1*$^{-/-}$ mice phenocopied many aspects of SIRT1 activation, such as a higher mitochondrial content, increased energy expenditure, and protection against metabolic disease. Also, the pharmacologic inhibition of PARP *in vitro* and *in vivo* increased $NAD^+$ content, SIRT1 activity and enhanced oxidative metabolism. These data show how PARP-1 inhibition has strong metabolic implications through the modulation of SIRT1 activity, a property that not only could be useful in the management of metabolic diseases but also of cancer.

### Keywords

caloric restriction; longevity; mitochondria; $NAD^+$; oxidative phosphorylation; peroxisome proliferator activated receptor gamma coactivator 1α; poly(ADP-ribose) polymerase; SIRT1



*Correspondence should be sent to: Johan Auwerx, M.D., Ph.D. at the Laboratory of Integrative and Systems Physiology, Ecole Polytechnique Fédérale de Lausanne (EPFL), SV-IBI, Building AI, Station 15, CH-1015 Lausanne, Switzerland Phone: +41-21-693 9522 Fax: +41-21-693 9600 admin.auwerx@epfl.ch.

The authors declare no conflict of interest.

## Introduction

Intracellular $NAD^+$ levels control the activity of the type III deacetylase SIRT1 allowing it to act both as a metabolic sensor and effector (Yu and Auwerx, 2009). Overexpression studies indicated how activation of SIRT1 or of its orthologs extends lifespan in lower eukaryotes and protects against high-fat diet (HFD)-induced metabolic disease in mice (Yu and Auwerx, 2009). These attractive properties spurred a quest to identify small molecule SIRT1 agonists that could be used in situations of metabolic stress and damage. This strategy identified compounds like resveratrol or SRT1720 (Howitz et al., 2003; Milne et al., 2007), whose ability to directly interact and activate SIRT1 is, however, debated (Pacholec et al., 2010). Therefore, a strong interest exists to develop alternative strategies to activate SIRT1. Given the $NAD^+$-dependency of SIRT1, another potential way to activate it is by increasing $NAD^+$ availability. This could be achieved by specifically inhibiting other $NAD^+$-consuming activities.

Poly(ADP-ribose) polymerase (PARP)-1 is a major cellular $NAD^+$ consumer (Sims et al., 1981). PARP-1 is activated upon binding to damaged or abnormal DNA (Durkacz et al., 1980), and catalyzes the formation of poly(ADP-ribose) polymers (PAR) onto different acceptor proteins, including PARP-1 itself (auto-PARylation), using $NAD^+$ as substrate (Adamietz, 1987). PARP-1 activation depletes cellular $NAD^+$ levels, using it to form PAR (Sims et al., 1981). This led us to test the influence of PARP-1 on SIRT1 activity and metabolic homeostasis. Our results show how a reduction/ablation of PARP-1 activity boosts $NAD^+$ levels and SIRT1 activity, which, in turn, enhances mitochondrial content and function, culminating in a solid protection against metabolic disease.

## Results

### PARP-$1^{-/-}$ mice are leaner and have increased energy expenditure

Chow fed *PARP-*$1^{-/-}$ mice (Menissier-de Murcia et al., 1997) weighed less (Fig.1A) and accumulated less fat than *PARP-*$1^{+/+}$ littermates upon aging (Fig.1B) despite eating significantly more (Fig.1C). During indirect calorimetry, *PARP-*$1^{-/-}$ mice consumed more $O_2$ (Fig.1D), suggestive of higher energy expenditure (EE). Resting EE was not different (Fig.S1A), indicating that the increase was due to changes at night, when mice are active. Accordingly, *PARP-*$1^{-/-}$ mice were more active at night (Fig.S1B). In addition, the respiratory quotient was also higher in *PARP-*$1^{-/-}$ mice during the dark phase, indicating enhanced glucose oxidation during the feeding period (Fig.1E). *PARP-*$1^{-/-}$ mice also maintained a higher body temperature upon cold exposure (Fig.1F), were more glucose tolerant (Fig.1G) and had a trend towards lower fasting blood glucose levels (4.30±0.17 mM in *PARP-*$1^{+/+}$ mice vs. 3.98±0.18 mM in *PARP-*$1^{-/-}$ mice; $p$=0.058), despite similar insulin levels (data not shown). During euglycemic-hyperinsulinemic clamp, glucose infusion rates or hepatic glucose production were similar to *PARP-*$1^{+/+}$ mice, but supporting their better glucose tolerance, glucose uptake in *PARP-*$1^{-/-}$ muscle trended up (Fig.S1C-E). In line with the lower fat mass and improved glucose tolerance, serum triglycerides (1.04±0.07 mM in *PARP-*$1^{+/+}$ vs. 0.84±0.05 mM in *PARP-*$1^{-/-}$ mice; $p$=0.048) and free fatty acids (FFA) (0.93±0.09 mEq/L in *PARP-*$1^{+/+}$ vs. 0.72±0.03 mEq/L in *PARP-*$1^{-/-}$ mice; $p$=0.040) were reduced in *PARP-*$1^{-/-}$ mice.

### PARP-1 is induced by nutrient availability and contributes to HFD-induced diabesity

The metabolic impact of *PARP-1* deletion made us evaluate whether nutrient scarcity (fasting) or overload (HFD) affects PARP-1 activity. Despite similar PARP-1 protein levels, a 24-hr fast sharply reduced PARP-1 autoPARylation levels, which reflect global PARP activity (Adamietz, 1987), suggesting a lower enzymatic activity (Fig.1H). In contrast, HFD

robustly increased PARP-1 protein levels and activity (Fig.1I), indicating a positive correlation between PARP-1 activity and nutrient availability.

As nutrient availability induces PARP-1 activity and *PARP-1* deletion prompts a leaner phenotype, we next explored how *PARP-1*$^{-/-}$ mice responded to HFD-induced metabolic disease. *PARP-1*$^{-/-}$ mice gained less weight after 2 months of HFD (Fig.1J), due to a lower fat accumulation (Fig.S1F). Moreover, *PARP-1*$^{-/-}$ mice on HFD were more glucose tolerant (Fig.1K), insulin sensitized (Fig.1L), and had lower serum FFAs (0.66±0.05 mEq/L vs. 0.53±0.03 mEq/L; $p$=0.026).

## Mitochondrial activation in brown adipose tissue and muscle from PARP-1$^{-/-}$ mice

The above results suggested improved mitochondrial activity in key metabolic tissues of *PARP-1*$^{-/-}$ mice, such as skeletal muscle and brown adipose tissue (BAT). *PARP-1*$^{-/-}$ mice had a relative higher amount of BAT, with a more intense red appearance (Fig.S1G). Transmission electron microscopy revealed higher mitochondrial content in *PARP-1*$^{-/-}$ BAT (Fig.1M), which was further corroborated by the increased mitochondrial DNA content (Fig.S1H) and mRNA expression of genes involved in mitochondrial respiration (*Ndufa2*, *Ndufb2*, *Ndufb5*, *Cyt C*, *COX17*), uncoupling (*UCP1*, *UCP3*), fatty acid oxidation (*MCAD)*, and thyroid hormone activation (*Dio2*). Mitochondrial biogenesis was also evidenced by the higher protein content of subunits from different respiratory complexes in the BAT from *PARP-1*$^{-/-}$ mice (Fig.10).

Also *PARP-1*$^{-/-}$ skeletal muscle had a marked oxidative profile. Succinate dehydrogenase (SDH) staining (Fig.1P) and the expression of muscle fiber isotype genes (*Trop I*, *MHCI*) (Fig.1Q) exposed an increase in oxidative fibers with a high mitochondrial content. As in BAT, the increased mitochondrial content was linked to an induction of the mRNA (Fig.1Q) and protein levels (Fig.1R) of mitochondrial components. In contrast to BAT and muscle, the expression of key metabolic genes was not altered in *PARP-1*$^{-/-}$ livers (Fig.S1I), reflecting a minor role of PARP-1 in the liver, probably due to its very low expression (Fig.S1J).

## Higher NAD$^+$ content and SIRT1 activity in BAT and muscle from PARP-1$^{-/-}$ mice

The *PARP-1*$^{-/-}$ mice phenocopy many features seen after SIRT1 activation (Yu and Auwerx, 2009). As PARP-1 is a major NAD$^+$-consumer (Sims et al., 1981), we speculated that the lack of PARP-1 activity might increase NAD$^+$ content, in turn activating SIRT1. Illustrating how PARP-1 drives most PARP activity, the ablation of *PARP-1* reduced PARylation in both BAT and muscle (Fig.2A). The expression of the other PARP enzymes was not increased in *PARP-1*$^{-/-}$ BAT and muscle (Fig.S2A-B), explaining the lack of compensation on PARylation. Confirming previous studies (Allinson et al., 2003; Fong et al., 2009), terminal dUTP nick-end labeling indicated that DNA damage was not increased in *PARP-1*$^{-/-}$ tissues (data not shown). In line with the attenuated NAD$^+$-consuming PARP activity, NAD$^+$ content was robustly increased in *PARP-1*$^{-/-}$ BAT and muscle (Fig.2B), while the levels of nicotinamide (NAM), a NAD$^+$-derived metabolite that inhibits sirtuin activity (Bitterman et al., 2002), remained unaffected (Fig.2C).

We next tested if the increase in NAD$^+$ correlated with SIRT1 activation. Indicative of SIRT1 activation, and supporting the higher mitochondrial content, PGC-1α acetylation levels in BAT and muscle of *PARP-1*$^{-/-}$ mice were reduced by ~40% and ~90%, respectively (Fig.2D-E). The acetylation of another SIRT1 target, forkhead box O1 (FOXO1), was also reduced by ~60% in BAT and ~40% in muscle (Fig.2D-E), supporting that *PARP-1* deficiency leads to SIRT1 activation. Remarkably, SIRT1 protein was also

robustly induced in *PARP-1*$^{-/-}$ BAT and muscle (Fig.2D-E), further amplifying SIRT1 activity.

As altered $NAD^+$ levels could also potentially impact on other sirtuins, we also tested the activity of SIRT2 and SIRT3, which act as cytoplasmic and mitochondrial sirtuins, respectively. The acetylation level of tubulin, a SIRT2 target (North et al., 2003), was not altered in muscle from *PARP-1*$^{-/-}$ mice (Fig.2F). Likewise, the acetylation of Complex I, a target for SIRT3 (Ahn et al., 2008) even showed a slight tendency to increase in *PARP-1*$^{-/-}$ muscles (Fig.2G). These results indicate that not all sirtuins are activated in *PARP-1*$^{-/-}$ tissues.

## Reduced PARP-1 activity in cellular models enhances oxidative metabolism

Next, we knocked-down *PARP-1* in HEK293T cells to evaluate whether an acute reduction in PARP-1 activity enhances oxidative metabolism. In these conditions, PARP-1 protein levels were reduced by ~80% and the low PARP1 auto-PARyation demonstrated that PARP activity was largely blunted (Fig.3A). The reduced PARP activity was associated with enhanced $NAD^+$ content and SIRT1 function, as illustrated by decreased PGC-1α acetylation (Fig.3B-C). Importantly, this happened despite unchanged SIRT1 protein levels (Fig.3C) or changes in the activity of SIRT2 or SIRT3, as manifested in tubulin, Ndufa9 or total mitochondrial acetylation levels (Fig.S3A-C). The induction of SIRT1 and PGC-1α activity culminated in a robust increase in mitochondrial DNA content (Fig.3D), mitochondrial-related gene expression (Fig.3E), and $O_2$ consumption (Fig.3F). Importantly, most of the metabolic effects elicited by PARP-1 depletion were lost when SIRT1 was simultaneously knocked-down (Fig.3D-F).

In line with the results in HEK293T cells, the expression of genes involved in mitochondrial function, mitochondrial DNA content and $O_2$ consumption were also induced in *PARP-1*$^{-/-}$ compared to *PARP-1*$^{+/+}$ MEFs (Fig.S3D-F). In line with our observations in tissues from *PARP-1*$^{-/-}$ mice, SIRT1 protein was also induced in *PARP-1*$^{-/-}$ MEFs (Fig.S3G).

## Pharmacological PARP inhibition enhances oxidative metabolism via SIRT1

To test the relation between SIRT1 and PARP-1 activities, we exposed C2C12 myotubes to $H_2O_2$ (500 μM, 6h), a well-known inducer of PARP-1 activity (Schraufstatter et al., 1986). $H_2O_2$ treatment vigorously increased PARP-1 (Fig.4A) and global protein PARylation levels (Fig.4B), as manifested by the slow migrating bands, in the absence of changes in PARP-1 levels (Fig.4A-B). Importantly, SIRT1 was not PARylated in response to $H_2O_2$ (Fig.4A), indicating that it is not a PARylation substrate. As reported (Schraufstatter et al., 1986), the $H_2O_2$-induced increase in PARP-1 activity sharply depleted $NAD^+$ content (Fig. 4C), but did not affect SIRT1 protein levels (Fig.4A-B). This lower $NAD^+$ availability limited SIRT1 activity, as reflected in PGC-1α hyperacetylation (Fig.4D). Interestingly, the inhibition of PARP activity with PJ34 (Garcia et al., 2001) rescued the drop in $NAD^+$ and recovered SIRT1 function during $H_2O_2$ exposure (Fig.4B-D). These results indicate that PARP-1 activation restrains SIRT1 activity and that PARP inhibitors relieve this limitation.

PARP-1 activity is not necessarily linked to DNA-damage and it has been shown to fluctuate in a circadian fashion (Asher et al., 2010). Therefore, we wondered whether prolonged PARP inhibition, even in the absence of DNA damage, would favor $NAD^+$ accumulation and, potentially, SIRT1 activity. Supporting this premise, PARP inhibition by PJ34 (Fig.4E) or a structurally unrelated compound, TIQ-A (data not shown), gradually raised $NAD^+$ levels, becoming significant after 24hr. At that time, PARP activity, but not PARP-1 protein levels, was robustly decreased (Fig.4F). PJ34 increased $NAD^+$ levels dose-dependently, in correlation with SIRT1 activity, as illustrated by PGC-1α deacetylation (Fig.

4G). Similar effects also happened *in vivo*, as treatment of mice with PJ34 (10 mg/kg, BID for 5 days) blunted basal PARP activity in muscle (Fig. 4H), while increasing $NAD^+$ and SIRT1 activity (Fig.4I). Despite the short duration of the treatment, serum triglyceride (1.21±0.08 mM Vehicle vs. 1.11±0.04 mM PJ34; $p$=0.08) and FFA levels (1.59±0.06 mEq/L vehicle vs. 1.44±0.03 mEq/L PJ34; $p$=0.03) were reduced in PJ34-treated mice. Of note, while compounds like resveratrol impact on SIRT1 through AMP-activated protein kinase (AMPK) (Canto et al., 2010), PJ34 did not alter AMPK activity, as reflected by the unchanged acetyl-CoA carboxylase (ACC) phosphorylation in either C2C12 myotubes (Fig. 4J) or gastrocnemius muscle (Fig.4H). PJ34 neither affected SIRT1 protein levels (Fig. 4H and 4J), but robustly induced the expression of mitochondrial and lipid oxidation genes both in C2C12 myotubes and muscle (Fig.4K-L). This was consistent with PJ34-induced PGC-1α activation and its recruitment to target gene promoters (e.g. *PDK4*; Fig.1A) and culminated in higher $O_2$ consumption rates (Fig.4M), testifying for enhanced oxidative metabolism.

The effect of PJ34 on PGC-1α acetylation in C2C12 myotubes was blunted upon *SIRT1* knock-down (Fig.4J). The role of SIRT1 in mediating PJ34-induced PGC-1α deacetylation was further confirmed in *SIRT1*$^{-/-}$ MEFs, where PJ34 was unable to decrease PGC-1α acetylation (Fig.S4B). In line with impaired PGC-1α activation, mitochondrial gene expression and $O_2$ consumption, were largely unresponsive to PJ34 upon SIRT1 depletion in C2C12 cells (Fig. 4K and 4M) and in *SIRT1*$^{-/-}$ MEFs (Fig.S4C-D), indicating that SIRT1 is a key mediator of PJ34 action. However, PJ34 also had SIRT1-independent effects, as reflected by the persistent increase in *UCP3* mRNA even after the *SIRT1* knock-down (Fig. 4K). This could be explained by the fact that PJ34 does not regulate *UCP3* expression by recruitment of PGC-1α to its promoter (Fig.S4A). The pharmacological inhibition of PARP recapitulates the phenotypic characteristics of the *PARP-1*$^{-/-}$ mice, and reveals that these effects are largely mediated by SIRT1.

## Discussion

The difficulty to identify compounds that specifically and directly bind and activate SIRT1 led us to test whether the modulation of $NAD^+$ availability could be an alternative path to activate SIRT1. Our present work supports this concept by showing how the attenuation of PARP-1, another $NAD^+$-consuming enzyme, increases intracellular $NAD^+$ levels and enhances SIRT1 activity. This prompts the deacetylation and activation of key metabolic transcriptional regulators such as PGC-1α and FOXO1, leading to increased mitochondrial content and metabolism.

Our data suggests that PARP-1 limits $NAD^+$ availability for SIRT1 activation. This concept originates from the differences in the $K_M$ and $K_{cat}/K_M$ of both enzymes for $NAD^+$, which indicate that PARP-1 is a faster and more efficient $NAD^+$ consumer than SIRT1 (Knight and Chambers, 2001; Smith et al., 2009). Therefore, it is likely that PARP-1 activity maintains $NAD^+$ at limiting levels for SIRT1 function. The prediction that *PARP-1* deletion would increase $NAD^+$ levels and activate SIRT1 is perfectly matched by our data. While previous work already speculated on a link between PARP-1 and sirtuin activities (Kolthur-Seetharam et al., 2006; Pillai et al., 2005), our study expands the consequences of this link to energy homeostasis. In apparent discrepancy, one report (Devalaraja-Narashimha and Padanilam, 2010) suggested that *PARP-1*$^{-/-}$ mice could be more susceptible to HFD-induced obesity. However, that study used mice on an SV129 background, which are less suited for metabolic studies than C57Bl/6J mice. The convergent results of our genetic, physiological, pharmacological and in vitro studies clearly support our conclusions.

Results from our lab indicate that the activation of SIRT1 after a bout of exercise or cold exposure is not linked to decreased PARP-1 activity (data not shown). Rather, only robust

and/or protracted changes, such as pharmacological (PJ34) or genetic (knock-down or deletion) PARP-1 inhibition, influence SIRT1 activity. While PARP-1 might not always participate in the physiological modulation of SIRT1 activity, our data suggest that the interplay between both proteins could be exploited pharmacologically.

Our work illustrates how SIRT1 is a key mediator of the PARP-1 deficient phenotype, but the link between PARP-1 and SIRT1 activities is still unclear. Several models used in this work show that reducing PARP-1 activity controls SIRT1 function independent of changes in SIRT1 protein levels. In all these cases, the levels of $NAD^+$, the rate-limiting coenzyme for SIRT1, correlated with SIRT1 activity, suggesting that $NAD^+$ availability might influence SIRT1 activity. If it were true, boosting $NAD^+$ content through alternative strategies should elicit similar metabolic phenotypes to those of the *PARP-1*$^{-/-}$ mice. Supporting this notion, the deletion of another $NAD^+$ consumer, CD38, also activates SIRT1 (Aksoy et al., 2006), resulting in protection against HFD-induced obesity (Barbosa et al., 2007). Nutrient scarcity and AMPK activation also lead to increased $NAD^+$ levels and SIRT1 activation coupled to the induction of oxidative metabolism (Canto et al., 2009; Canto et al., 2010). This correlative evidence indicates that the increased $NAD^+$ availability might be a key mechanism by which PARP deficiency activates SIRT1. However, we cannot exclude the possibility that PARP inhibition also impacts on SIRT1 via other means, even though our results rule out direct PARylation of SIRT1 as the mechanism (Fig.4A). In addition, SIRT1 content was also increased in *PARP-1*$^{-/-}$ tissues and MEFs, further amplifying SIRT1 activity. The reason for this increase in SIRT1 levels remains elusive, but is independent of changes in SIRT1 mRNA (PB, CC and JA, unpublished observations).

Of note, *PARP-1* depletion affects the activity of SIRT1, but not that of SIRT2 and SIRT3, which occupy non-nuclear compartments. If increased SIRT1 activity was mainly driven by changes in $NAD^+$, the unchanged SIRT2 and SIRT3 activities in *PARP-1*$^{-/-}$ tissues suggest that the increase in $NAD^+$ is either not enough to enhance SIRT2 and SIRT3 activities, or that it only happens in specific cellular compartments, supporting an independent regulation of different subcellular $NAD^+$ pools (Yang et al., 2007). Alternatively, PARP-1 and SIRT1 activities might not be linked by changes in $NAD^+$ and some yet unfound mechanism drives the specificity towards this sirtuin.

Some results indicate that the effects of PARP deficiency cannot be completely explained by SIRT1 (Fig.4K). Future research will have to clarify the nature of these SIRT1-independent effects of PARP inhibition on metabolism. It will be interesting to explore whether PARylation can directly modulate the activity of key metabolic transcriptional regulators, as PARP-1 may contribute to nuclear processes other than DNA repair (Krishnakumar and Kraus, 2010). PARP inhibitors are currently in clinical development as anti-tumoral drugs (Fong et al., 2009). While our data encourages a possible utilization of PARP inhibitors as therapeutic agents to activate SIRT1 and promote oxidative metabolism, this should be taken cautiously.

PARP-1 has key roles in genomic maintenance, and, while neither this nor previous studies (Allinson et al., 2003) detected enhanced DNA damage in *PARP-1*$^{-/-}$ mice under basal conditions, it cannot be ignored that *PARP-1*$^{-/-}$ mice are sensitive to ionizing radiation (Menissier-de Murcia et al.,1997). Hence, it will be important to analyze how ageing and metabolic disease impact on DNA damage to establish the therapeutic potential and limitations of PARP inhibition.

## Experimental procedures

Detailed materials and procedures can be found as supplemental information.

### Animal experiments

Pure C57Bl/6J male mice were used for the study. *PARP-1*$^{+/+}$ and *PARP-1*$^{-/-}$ were described (Menissier-de Murcia et al., 1997). Mice were housed separately, had *ad libitum* access to water and chow (10 kcal% of fat, *Safe*, Augy, France) or HFD (60 kcal% of fat, *Research Diets*, New Brunswick, NJ, USA), and were kept under a 12h dark-light cycle. Animal experiments were carried out according to local national and EU ethical guidelines. Animals were sacrificed after a 6h of fast, and tissues were collected and processed as specified.

### $NAD^+$ and NAM determination

$NAD^+$ levels in cultured cells were determined using an enzymatic method (*Enzychrom*, BioAssays Systems, CA), whereas for tissues (Fig.4) $NAD^+$ and NAM levels were determined as described (Sauve et al., 2005).

### Statistics

All data was verified for normal distribution. Statistical significance was assessed by Student's t-test for independent samples. Values are expressed as mean +/− SEM unless otherwise stated.

## Supplementary Material

Refer to Web version on PubMed Central for supplementary material.

## Acknowledgments

This work was supported by fellowships by of Bolyai (PB), SNSF (PB), EMBO (CC), FEBS (AB) and NWO (RHH) as well as grants from the NKTH, OTKA (NFF78498, IN80481), Mecenatura (DE OEC Mec-1/2008), the NIH (DK59820), the ERC (2008-AdG-23118), the CNRS and the ANR.

## References

Adamietz P. Poly(ADP-ribose) synthase is the major endogenous nonhistone acceptor for poly(ADP-ribose) in alkylated rat hepatoma cells. Eur J Biochem. 1987; 169:365–372. [PubMed: 3121314]

Ahn BH, Kim HS, Song S, Lee IH, Liu J, Vassilopoulos A, Deng CX, Finkel T. A role for the mitochondrial deacetylase Sirt3 in regulating energy homeostasis. Proc Natl Acad Sci U S A. 2008; 105:14447–14452. [PubMed: 18794531]

Aksoy P, Escande C, White TA, Thompson M, Soares S, Benech JC, Chini EN. Regulation of SIRT 1 mediated NAD dependent deacetylation: a novel role for the multifunctional enzyme CD38. Biochem Biophys Res Commun. 2006; 349:353–359. [PubMed: 16935261]

Allinson SL, Dianova II, Dianov GL. Poly(ADP-ribose) polymerase in base excision repair: always engaged, but not essential for DNA damage processing. Acta Biochim Pol. 2003; 50:169–179. [PubMed: 12673357]

Asher G, Reinke H, Altmeyer M, Gutierrez-Arcelus M, Hottiger MO, Schibler U. Poly(ADP-ribose) polymerase 1 participates in the phase entrainment of circadian clocks to feeding. Cell. 2010; 142:943–953. [PubMed: 20832105]

Barbosa MT, Soares SM, Novak CM, Sinclair D, Levine JA, Aksoy P, Chini EN. The enzyme CD38 (a NAD glycohydrolase, EC 3.2.2.5) is necessary for the development of diet-induced obesity. Faseb J. 2007; 21:3629–3639. [PubMed: 17585054]

Bitterman KJ, Anderson RM, Cohen HY, Latorre-Esteves M, Sinclair DA. Inhibition of silencing and accelerated aging by nicotinamide, a putative negative regulator of yeast sir2 and human SIRT1. J Biol Chem. 2002; 277:45099–45107. [PubMed: 12297502]

Canto C, Gerhart-Hines Z, Feige JN, Lagouge M, Noriega L, Milne JC, Elliott PJ, Puigserver P, Auwerx J. AMPK regulates energy expenditure by modulating NAD+ metabolism and SIRT1 activity. Nature. 2009; 458:1056–1060. [PubMed: 19262508]

Canto C, Jiang LQ, Deshmukh AS, Mataki C, Coste A, Lagouge M, Zierath JR, Auwerx J. Interdependence of AMPK and SIRT1 for metabolic adaptation to fasting and exercise in skeletal muscle. Cell Metab. 2010; 11:213–219. [PubMed: 20197054]

Devalaraja-Narashimha K, Padanilam BJ. PARP1 deficiency exacerbates diet-induced obesity in mice. J Endocrinol. 2010; 205:243–252. [PubMed: 20338998]

Durkacz BW, Omidiji O, Gray DA, Shall S. (ADP-ribose)n participates in DNA excision repair. Nature. 1980; 283:593–596. [PubMed: 6243744]

Fong PC, Boss DS, Yap TA, Tutt A, Wu P, Mergui-Roelvink M, Mortimer P, Swaisland H, Lau A, O'Connor MJ, et al. Inhibition of Poly(ADP-Ribose) Polymerase in Tumors from BRCA Mutation Carriers. N Engl J Med. 2009; 24:24.

Garcia SF, Virag L, Jagtap P, Szabo E, Mabley JG, Liaudet L, Marton A, Hoyt DG, Murthy KG, Salzman AL, et al. Diabetic endothelial dysfunction: the role of poly(ADP-ribose) polymerase activation. NatMed. 2001; 7:108–113.

Howitz KT, Bitterman KJ, Cohen HY, Lamming DW, Lavu S, Wood JG, Zipkin RE, Chung P, Kisielewski A, Zhang LL, et al. Small molecule activators of sirtuins extend Saccharomyces cerevisiae lifespan. Nature. 2003; 425:191–196. [PubMed: 12939617]

Knight MI, Chambers PJ. Production, extraction, and purification of human poly(ADP-ribose) polymerase-1 (PARP-1) with high specific activity. Protein Expr Purif. 2001; 23:453–458. [PubMed: 11722183]

Kolthur-Seetharam U, Dantzer F, McBurney MW, de Murcia G, Sassone-Corsi P. Control of AIF-mediated cell death by the functional interplay of SIRT1 and PARP-1 in response to DNA damage. Cell Cycle. 2006; 5:873–877. [PubMed: 16628003]

Krishnakumar R, Kraus WL. The PARP side of the nucleus: molecular actions, physiological outcomes, and clinical targets. Mol Cell. 2010; 39:8–24. [PubMed: 20603072]

Menissier-de Murcia J, Niedergang C, Trucco C, Ricoul M, Dutrillaux B, Mark M, Oliver FJ, Masson M, Dierich A, LeMeur M, et al. Requirement of poly(ADP-ribose) polymerase in recovery from DNA damage in mice and in cells. ProcNatlAcadSciUSA. 1997; 94:7303–7307.

Milne JC, Lambert PD, Schenk S, Carney DP, Smith JJ, Gagne DJ, Jin L, Boss O, Perni RB, Vu CB, et al. Small molecule activators of SIRT1 as therapeutics for the treatment of type 2 diabetes. Nature. 2007; 450:712–716. [PubMed: 18046409]

North BJ, Marshall BL, Borra MT, Denu JM, Verdin E. The human Sir2 ortholog, SIRT2, is an NAD +-dependent tubulin deacetylase. Mol Cell. 2003; 11:437–444. [PubMed: 12620231]

Pacholec M, Bleasdale JE, Chrunyk B, Cunningham D, Flynn D, Garofalo RS, Griffith D, Griffor M, Loulakis P, Pabst B, et al. SRT1720, SRT2183, SRT1460, and resveratrol are not direct activators of SIRT1. J. 2010; 285:8340–8351.

Pillai JB, Isbatan A, Imai S, Gupta MP. Poly(ADP-ribose) polymerase-1-dependent cardiac myocyte cell death during heart failure is mediated by NAD+ depletion and reduced Sir2alpha deacetylase activity. JBiolChem. 2005; 280:43121–43130.

Sauve AA, Moir RD, Schramm VL, Willis IM. Chemical activation of Sir2-dependent silencing by relief of nicotinamide inhibition. Mol Cell. 2005; 17:595–601. [PubMed: 15721262]

Schraufstatter IU, Hinshaw DB, Hyslop PA, Spragg RG, Cochrane CG. Oxidant injury of cells. DNA strand-breaks activate polyadenosine diphosphate-ribose polymerase and lead to depletion of nicotinamide adenine dinucleotide. J Clin Invest. 1986; 77:1312–1320. [PubMed: 2937805]

Sims JL, Berger SJ, Berger NA. Effects of nicotinamide on NAD and poly(ADP-ribose) metabolism in DNA-damaged human lymphocytes. J Supramol Struct Cell Biochem. 1981; 16:281–288. [PubMed: 6458707]

Smith BC, Hallows WC, Denu JM. A continuous microplate assay for sirtuins and nicotinamide-producing enzymes. Anal Biochem. 2009; 394:101–109. [PubMed: 19615966]

Yang H, Yang T, Baur JA, Perez E, Matsui T, Carmona JJ, Lamming DW, Souza-Pinto NC, Bohr VA, Rosenzweig A, et al. Nutrient-sensitive mitochondrial NAD+ levels dictate cell survival. Cell. 2007; 130:1095–1107. [PubMed: 17889652]

Yu J, Auwerx J. The role of sirtuins in the control of metabolic homeostasis. Ann N Y Acad Sci. 2009; 1173(Suppl 1):E10–19. [PubMed: 19751409]

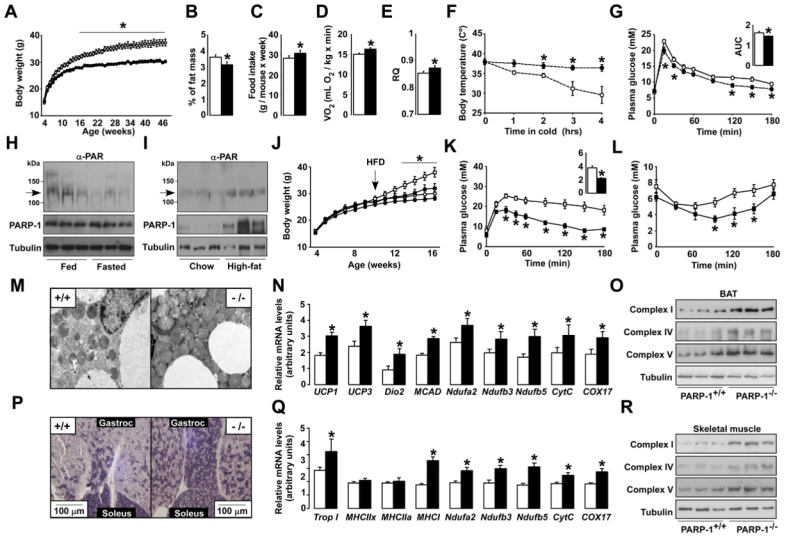


**Figure 1. Phenotyping the PARP-1$^{-/-}$ mice**

**(A**) Body weight (BW) evolution in *PARP-1*$^{+/+}$ and $^{-/-}$ mice (n=8/9). **(B)** Epididymal white adipose tissue mass. **(C)** Average food consumption. **(D)** $O_2$ consumption and **(E)** respiratory quotient (RQ) of *PARP-1*$^{+/+}$ and $^{-/-}$ mice (n=9/9) determined by indirect calorimetry. **(F)** Body temperature after exposure to 4°C (n=6/5). **(G)** Oral glucose tolerance test (OGTT) (n=5/5) and the area under curve (AUC). **(H)** PARP-1 autoPARylation (arrow), analyzed in 100µg of protein extract from gastrocnemius muscles of 16 wk-old mice fed ad libitum or fasted (24h). PARP-1 and tubulin levels were checked using 50µg of protein extract. (**I)** Gastrocnemius from mice on CD or HFD (12 wk) were analyzed as in (H). **(J)** BW evolution in *PARP-1*$^{+/+}$ and $^{-/-}$ mice (n=10/10) fed a CD (circles) or HFD (squares) from 8 wk of age. **(K)** OGTT and **(L)** an insulin tolerance test in HFD fed *PARP-1*$^{+/+}$ and $^{-/-}$ mice at 16 wk of age (n=10/10). The AUC of the OGTT is shown on the top-right. (**M-O)** BAT from *PARP-1*$^{+/+}$ and $^{-/-}$ mice on CD was extracted and mitochondrial biogenesis was analyzed by (M) transmission electron microscopy, (N) mRNA expression of the genes indicated and (O) the abundance of mitochondrial complexes in 25µg of total protein extracts. **(P)** SDH staining of sections from gastrocnemius and soleus of *PARP-1*$^{+/+}$ and $^{-/-}$ mice on CD. **(Q-R)** Gastrocnemius was also used to analyze mRNA levels of the indicated genes (Q) and the abundance of mitochondrial complexes in 25µg of total protein extracts (R). White bars represent *PARP-1*$^{+/+}$; black bars represent *PARP1*$^{-/-}$ mice. * indicates statistical difference vs. PARP-1$^{+/+}$ at $p<0.05$. For abbreviations, see Table S1.

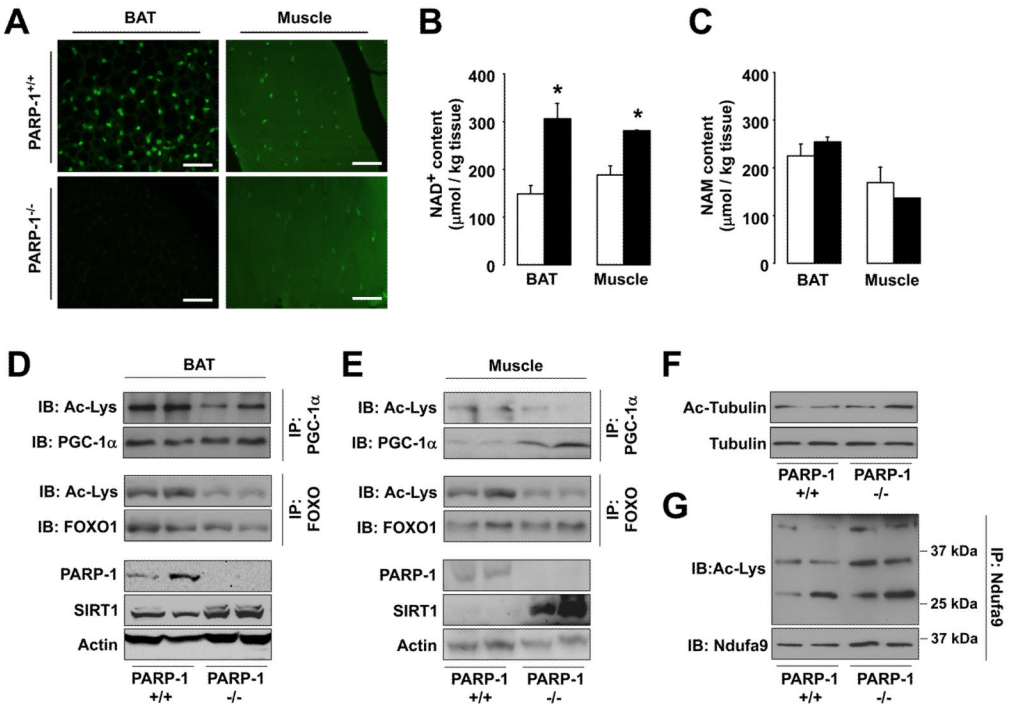


**Figure 2. PARP-1 deletion raises NAD$^+$ levels and activates SIRT1**

**(A)** Protein PARylation determined by α-PAR staining on formalin-fixed 7µm BAT and muscle tissue sections of *PARP-1*$^{+/+}$ and $^{-/-}$ mice. White bar = 10µm. **(B)** NAD$^+$ and **(C)** NAM levels in BAT and muscle from *PARP-1*$^{+/+}$ (white bars) and *PARP-1*$^{-/-}$ (black bars) mice determined by mass spectrometry. **(D-E)** PARP-1, SIRT1 and actin protein content in BAT (D) and muscle (E) were determined by Western blot, using 100µg of protein lysate. PGC-1α and FOXO1 acetylation were examined by immunoprecipitation. **(F)** Tubulin and acetylated-tubulin levels were tested in *PARP-1*$^{+/+}$ and $^{-/-}$ gastrocnemius. **(G)** The Ndufa9 subunit of mitochondrial complex I was immunoprecipitated from 400µg of total protein from gastrocnemius and acetylation levels were analyzed by Western blot. * indicates statistical difference vs. *PARP-1*$^{+/+}$ mice at $p<0.05$.

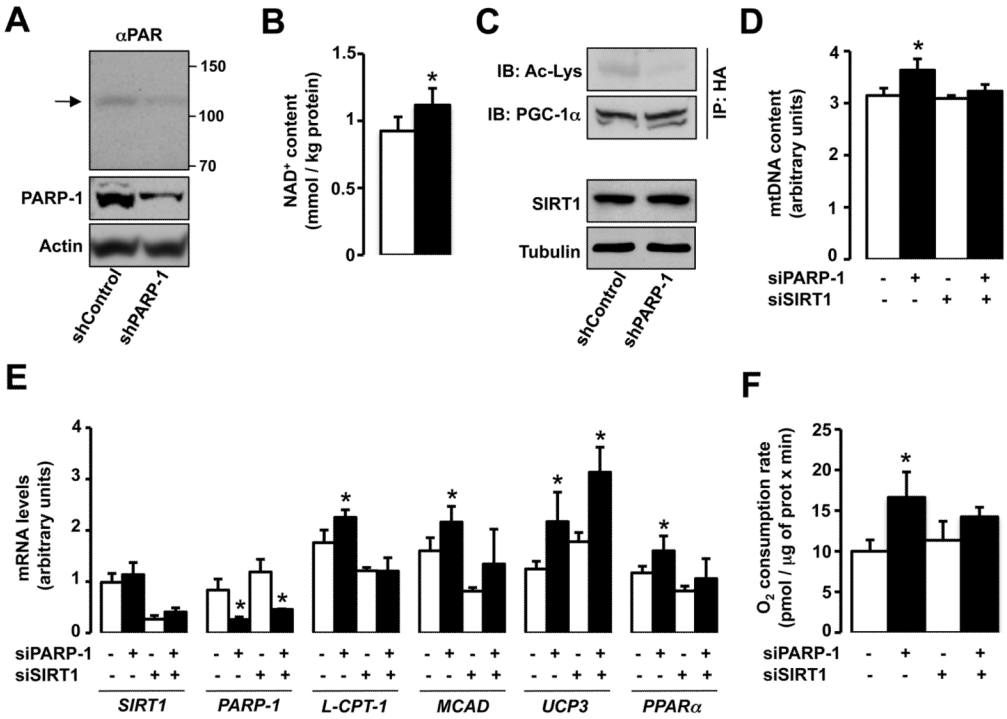


**Figure 3. PARP-1 knock-down promotes SIRT1 activity and oxidative metabolism**

**(A-C)** HEK293T cells were transfected with either scramble (control) or *PARP-1* shRNA and HA-PGC-1α expression vector for 48h. Then, (A) PARP-1 protein levels and autoPARylation (arrowhead) were analyzed in total protein lysates. (B) Intracellular $NAD^+$ was measured on total acid extracts. (C) PGC-1α acetylation was analyzed in HA immunoprecipitates. **(D-F)** HEK293T cells were transfected with either a pool of *PARP-1* siRNAs, a pool of *SIRT1* siRNAs, or different combinations of both using the corresponding scramble siRNAs as control (−). The cells were simultaneously transfected with HA-PGC-1α for 48h. Then, (D) relative mitochondrial DNA content, (E) mRNA levels of the genes indicated and (F) total $O_2$ consumption was analyzed. * indicates statistical difference vs. respective control sh/siRNA-transfected cells at $p<0.05$.

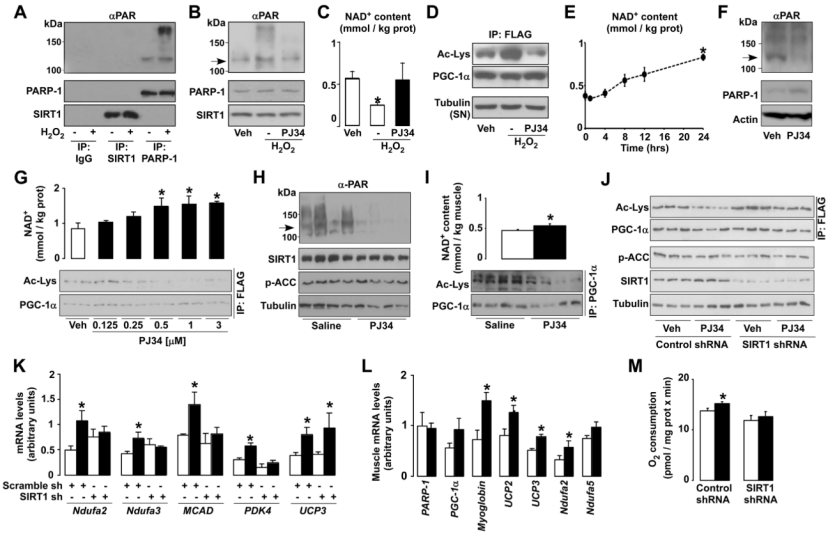


**Figure 4. PARP-1 inhibition enhances mitochondrial function through SIRT1**

**(A-C)** C2C12 myotubes expressing FLAG-HA-PGC-1α were treated for 6h with either PBS (vehicle (Veh)), $H_2O_2$ (500μM) or $H_2O_2$ and PJ34 (1μM). Then, (A) SIRT1, PARP-1 and unspecific IgG immunoprecipitates from 500 μg of protein extracts were used to test PARylation and the proteins indicated. (B) proteins were analyzed in total cell extracts and the arrow indicates PARP-1 autoPARylation. (C) $NAD^+$ content was measured and (D) PGC-1α acetylation was tested in FLAG immunoprecipitates. Tubulin was checked on the supernatants as input. **(E)** C2C12 myotubes were treated with PJ34 (1μM) for the times indicated and $NAD^+$ levels were evaluated in acidic extracts. **(F-G)** C2C12 myotubes expressing FLAG-HA-PGC-1α were treated for 24h with PBS (Veh) or with PJ34 (1 μM, unless stated). (F) PARP-1 protein and autoPARylation (arrow) were determined by Western blot and (G) $NAD^+$ content and PGC-1α acetylation were measured. **(H-I)** 10-wk old mice received PJ34 (10mg/kg BID i.p.) or saline (Veh) for 5 days before sacrifice (n=10/10); then (H) PARP-1 autoPARylation (arrow), p-ACC and SIRT1 levels were determined in 100μg of total protein extracts from gastrocnemius and (I) $NAD^+$ and PGC-1α acetylation were determined. PGC-1α was immunoprecipitated using 2mg of protein from gastrocnemius muscle and 5μg of antibody**. (J-K)** C2C12 myotubes expressing FLAG-HA-PGC-1α and either a control or a SIRT1 shRNA were treated with PJ34 for 48h. Then, (J) PGC-1α acetylation levels were quantified in FLAG immunoprecipitates and 50μg of total protein extracts were used to measure the other markers indicated; (K) mRNA levels of selected genes were quantified. **(L)** Mice were treated as in (H) and mRNA of selected genes was determined in gastrocnemius. **(M)** C2C12 were treated as in (J) and cellular $O_2$ consumption was measured. White bars represent Veh; black bars represent PJ34 treatment. * indicates statistical difference vs. Veh group at $p<0.05$. For abbreviations, see Table S1.